Reducing Uncertainties for Spatial Averaging at High Frequencies

David Sinden*, Srinath Rajagopal
Ultrasound and Underwater Acoustics,
National Physical Laboratory, Teddington, United Kingdom
*Email: david.sinden@npl.co.uk

N. Christopher Chaggares†, Guofeng Pang and Oleg Ivanytskyy
FujiFilm VisualSonics Inc., Toronto, Canada.
†Email: chris.chaggares@fujifilm.com

***Abstract*—Accurate characterization of ultrasound fields generated by diagnostic and therapeutic transducers is critical for patient safety. At high frequencies, spatial variations in the pressure over the surface of the measurement device will produce a different averaged value from that at the intended location. Using a small hydrophone as an idealised point device, this paper seeks to ascertain the spatial-averaging errors for a finite-area reference device along the beam axis in order to find the optimal measurement location.**

***Index Terms*—hydrophones, high-frequency calibrations, spatial-averaging, uncertainties**

I. Introduction

Detailed spatial resolution in imaging requires high frequencies. Indeed, clinical systems with centre frequencies up to 50MHz are available. However, at such frequencies, the accuracy in measurements may be compromised if the device may be of comparable size to, or larger than the smallest characteristic length scale of the wave. In such cases, spatial variations in the pressure over the surface of the measurement device will produce a different averaged value from that at the intended location, potentially underestimating the field strength. This is a complex phenomenona; dependent on the profile of the focal volume, which is determined by the focusing mechanism, frequency, drive, type of transducer etc.

Using a 20 μm hydrophone as an idealised point device, this paper seeks to ascertain the spatial-averaging error for a finite-area reference device and determine the optimal axial position for the location of the hydrophone so that the spatial-averaging error is minimized for a nonlinear field. The spatial-averaging error is defined as the normalised difference between the maximum pressure and the averaged pressure. The averaged pressure is defined as the mean of a number of measurements uniformly sampled over the area of the reference device using the point device.

II. Methods

A. Hydrophone Transfer Characteristics

The idealized point receiver hydrophone used in this study to investigate the spatial-averaging of the focused field by a finite-sized hydrophone was based on a custom membrane type device manufactured by FujiFilm VisualSonics Inc. (VSI), Canada. The fabrication details of the hydrophone can be found in [1]. The hydrophone was constructed from a poled 6 μm thick Polyvinylidene fluoride trifluoroethylene (PVDF-TrFE) sheet stretched over a 20 mm diameter circular frame.

The VSI hydrophone was calibrated via a comparison technique [2] using a commercial membrane hydrophone (UT1602, Precision Acoustics Ltd, UK) with a nominal active aperture of diameter of 0.2 mm. The calibration of UT1602 was traceable to a primary standard from 1 to 60 MHz [3] and was also predicted from 1 to 110 MHz using a one-dimensional analytical model [4]. The relationship between the measured and modelled response was obtained by minimizing

$$C\left(f\right) = \left(M\left(f\right) - M_{\mathrm{meas}}\left(f\right)\right)^2, \tag{1}$$

where f is the frequency in Hz, and $M(f)$ and $M_{\mathrm{meas}}(f)$ are the modelled and measured magnitude transfer functions of the hydrophone respectively in units of V/Pa. The cost function was minimized using the unconstrained multivariable function implemented within MATLAB (MathWorks, Natick, MA., USA).

The predicted response of the UT1602 hydrophone was then used to calibrate the VSI hydrophone from 4.5 to 110 MHz. For the calibration, a 5 MHz focused transducer, Table I, was excited by a tone burst drive voltage such that the field at the focus contained at least 20 harmonics of the fundamental frequency. The UT1602 hydrophone was first positioned and aligned for maximum signal in the plane perpendicular to the transducer axis using an 80 MHz high-pass filter, which isolated the high frequency components, thus improving the alignment sensitivity. Following the removal of the filter, the UT1602 output signal was measured over that region of the tone-burst for which a voltage waveform of constant amplitude was observed. The VSI hydrophone was then substituted at the same location and the procedure was repeated. The voltages from the two hydrophones were compared to derive the magnitude sensitivity, $M_{\mathrm{test}}(f)$, of the VSI hydrophone

$$M_{\mathrm{test}}(f) = M_{\mathrm{ref}}(f)\left|\mathcal{F}\left[v_{\mathrm{test}}\left(t\right)\right]/\mathcal{F}\left[v_{\mathrm{ref}}\left(t\right)\right]\right|, \tag{2}$$

978-1-5386-3383-0/17/$31.00 ©2017 IEEE

where $M_{\mathrm{ref}}(f)$ is the combined measured and predicted magnitude sensitivity of the UT1602 hydrophone up to 110 MHz, $v_{\mathrm{test}}(t)$ and $v_{\mathrm{ref}}(t)$ are the voltage responses of the VSI and UT1602 hydrophones respectively.

The measurements were repeated by driving the transducer at 4.5 and 5.5 MHz. The measured magnitude sensitivity was interpolated between 1 and 110 MHz in 1 MHz increments.

The phase response of a hydrophone can be derived by applying the minimum phase approximation [5], using only the magnitude response to derive the phase response, $\Phi_{\mathrm{test}}(f) = \mathcal{H}^{-1}\left[\ln\left(M_{\mathrm{test}}(f)\right)\right]$, where the phase is in radians and $\mathcal{H}[\cdot]$ is the Hilbert transform. The measured magnitude response of the VSI hydrophone and its phase response (derived using the minimum phase method) were used to deconvolve [6] the voltage signal into pressure.

In the comparison calibration technique, it was assumed that the spatial-averaging errors incurred by the VSI hydrophone were negligible. However, the area of the UT1602 hydrophone is a factor of around 100 times larger than the VSI device. Therefore the spatial-averaging errors need to be quantified in order to accurately estimate the magnitude sensitivity. The spatial-averaging correction of the UT1602 hydrophone was derived using the VSI hydrophone as an approximation to an idealized point receiver.

B. Spatial Averaging Corrections: Measurements

A 5 MHz focused transducer along with two other higher center frequency focused transducers (see Table I) were characterized using the VSI hydrophone in a beam plotting tank (UMS2, Precision Acoustics Ltd, Dorchester, UK) with seven degrees of freedom: manual tilt and rotation and three motorized axes for the transducer and manual tilt and rotation for the hydrophone. Bespoke software written in LabVIEW (National Instruments, Austin, Texas, USA) was used to post-process the waveforms acquired from the UMS2 software. The dimensions of the beam plotting tank are 1000×300×300 mm (L×W×H). Deionized (<6 μS.m^{-1}) and particulate (<1 μm) filtered water was used for measurements. All transducers were driven using a tone-burst signal consisting of 20 cycles at their respective drive voltages.

TABLE I: Single-element transducers tested.

Frequency (MHz)	Radius of Curvature (mm)	Diameter (mm)	F-number	Drive Voltage (Vpp)
5	59.7	9.5	6.3	200, 300
10	90	12.7	7.1	144
25	50	7	7.1	88

For each transducer, the focal peak was identified via an axial scan using the peak positive voltage of the hydrophone waveform. At the focal position, two scans were carried out

(i) an orthogonal scan ranging from at least -10 to 10 mm to determine the nature of the lateral extent of the focal field

(ii) a raster scan over an area of 1×1 mm in 25 μm steps, from which the spatial-averaging errors were derived.

The spatial-averaging correction $\delta_{\mathrm{meas}}(f)$ of a hydrophone with finite measurement area can be expressed as

$$\delta_{\mathrm{meas}}(f) = \left|\mathcal{F}\left[v_{\max}(t)\right] / \mathcal{F}\left[\hat{v}(t)\right]\right|, \tag{3}$$

where $v_{\max}(t)$ is the hydrophone waveform at the focal position and $\hat{v}(t)$ is the spatially-averaged waveform computed by using the raster scan waveforms centered from the position of $v_{\max}(t)$ such that they corresponded to the area represented by the finite sized hydrophone and $\mathcal{F}[\cdot]$ denotes the Fourier transform. The correction, $\delta_{\mathrm{meas}}(f)$, was applied by multiplying with the Fourier transform of the voltage $v_{\mathrm{ref}}(t)$ in Eq. (2).

C. Spatial Averaging Corrections: Simulations

As the acoustic field was generated by a weakly focused, axisymmetric transducer operating in a pseudo-continuous wave mode, the nonlinear acoustic field was modelled using Khokhlova-Zabolotskaya-Kuznetsov equation [7]. The field $p(r,z) = \sum_{i=1}^{N} p^{(i)}(r,z)$ was computed as the Fourier sum of it harmonic components, using an axisymmetric hybrid time and frequency domain code [8]. The code employs operator splitting; handling the nonlinear part in the time domain, using a hyperbolic conservation-law scheme and the attenuation and diffraction parts in the frequency domain. The numerical input power was matched against the experimental axial pressure data to compute the acousto-electrical efficiency of the system. The electric drive waveform supplied by the amplifier was measured and found to be sinusoidal. Thus, a single frequency Gaussian source boundary condition, along with perfectly matched layers on other boundaries were applied as boundary conditions. Simulations were performed for $N = 300$ harmonics, with over 500 points-per-wavelength, and a Courant-Friedrichs-Lewy number of 0.1 to ensure numerical stability.

From the computed acoustic field, at the axial maximum of the acoustic field, $z = z_{\max}$, the i^{th}-harmonic components, $p^{(i)}$, were averaged over the area, $A = \int_{\mathcal{A}(r)} \mathrm{d}r$, of the reference device

$$\hat{p}^{(i)} = \frac{1}{A}\int_{\mathcal{A}(r)} p^{(i)}\left(r, z_{\max}\right)\mathrm{d}r. \tag{4}$$

Then, the relative error, equivalent to the reciprocal (3), at each frequency is given by the averaged area and the maximum value of each harmonic within the area, which occurs at $r = r_{\max}$,

$$\varepsilon^{(i)} = \left|\hat{p}^{(i)} / p^{(i)}\left(r_{\max}, z_{\max}\right)\right|. \tag{5}$$

III. Results

A. Transfer Characteristics

The measured magnitude transfer function of the UT1602 hydrophone is traceable to the UK's primary standard for realising the acoustic pascal in water at megahertz frequencies [3] from 1 to 60 MHz and the predicted response using the hydrophone model [4] up to 110 MHz is shown in Fig. 1. The estimated model input parameters of the physical quantities

978-1-5386-3383-0/17/$31.00 ©2017 IEEE

returned by the minimization function for e.g., the piezoelectric coefficient, d_{33} with units of C/N and the characteristic electrical impedance in Ohms of the cable connecting the signal carrying electrode patterned on the membrane and the input of the preamplifier constitute the biggest uncertainties beyond the measured response. Though the values of the physical quantities returned from the optimization process lie within the known range of values, a higher uncertainty is ascertained in the modelled response since these could not be directly measured on the UT1602 hydrophone. Therefore, the uncertainties in the measured frequency range were used to linearly extrapolate the uncertainties in the modelled response and consequently, these were as high as 30% for frequencies in the range 61 to 110 MHz. The error bars are uncertainties expressed at 95% coverage probability.

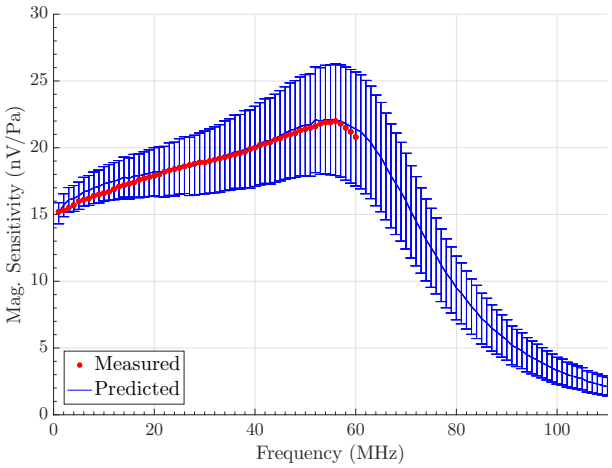

Fig. 1: Measured and predicted magnitude sensitivity of 0.2 mm diameter reference device.

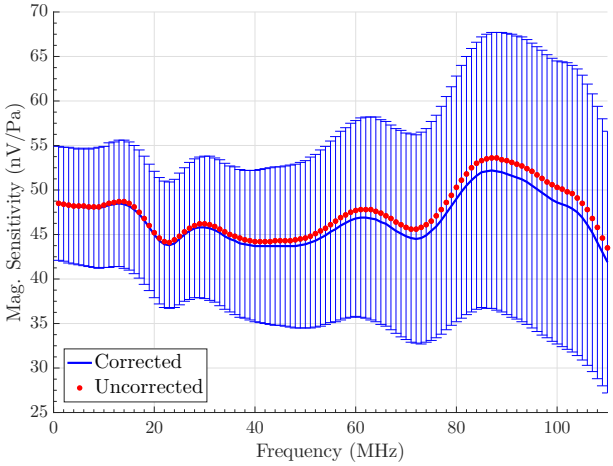

Fig. 2: Measured magnitude sensitivity of 20 μm test device, with and without spatial-averaging corrections applied to reference device.

The magnitude transfer function of the VSI hydrophone, derived using UT1602 as a reference hydrophone by the comparison technique is shown in Fig. 2. The uncertainty of the VSI hydrophone includes Type A random uncertainty and Type B systematic uncertainty contributions, which were combined according to [9]. The Type B contribution includes the uncertainty in the UT1602 hydrophone and the uncertainty in estimating the spatial-averaging corrections for UT1602 hydrophone relevant to the 5 MHz focused acoustic field used in this study.

B. Measured and Predicted Spatial Averaging Corrections

From the measured data for each transducer, the spatial-averaging errors were computed, relative to the local peak value, at the focal peak pressure over the diameter corresponding to the reference hydrophone, as illustrated in Fig. 3. The results are shown in Fig. 4, illustrating that the spatial-averaging error typically increases with frequency. There is good agreement for low harmonic components. The discrepancies at high-harmonic components can be attributed to the fact that the simulations are based on matching measured and simulated pressures fields, which are dominanted by the fundamental.

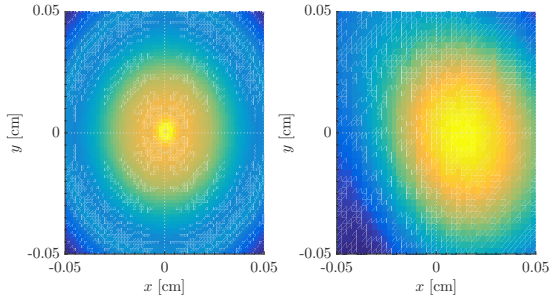

Fig. 3: Simulated and measured raster scans at the focal plane, over which spatial-averaging was performed, at 64 MHz. (Color schemes are normalised)

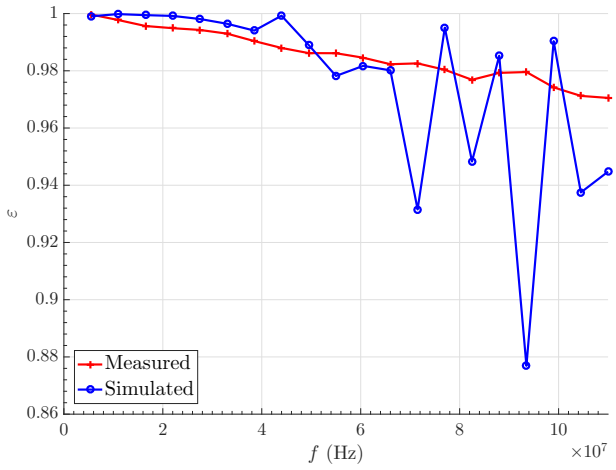

Fig. 4: Simulated and measured spatial-averaging errors at the focal plane of a 0.2 mm diameter hydrophone.

There are a number of reasons for the increase in the spatial-averaging error. Firstly, as the frequency increases and the

978-1-5386-3383-0/17/$31.00 ©2017 IEEE

wavelength decreases, so the potential for the spatial variation over the area of the hydrophone increases. Secondly, due to the effect of nonlinear propagation, the location of the peak for the acoustic fields from higher harmonic components will be post-focal. Thus, for higher-harmonic components, at the position at which measurements are taken, the field is not yet fully convergent. This is an artefact of generating high-frequency acoustic fields by nonlinear propagation.

For inter-comparisons between hydrophones, it is beneficial to minimize the spatial-averaging error. As Fig. 5 illustrates, this can be achieved by acquiring data post-focally.

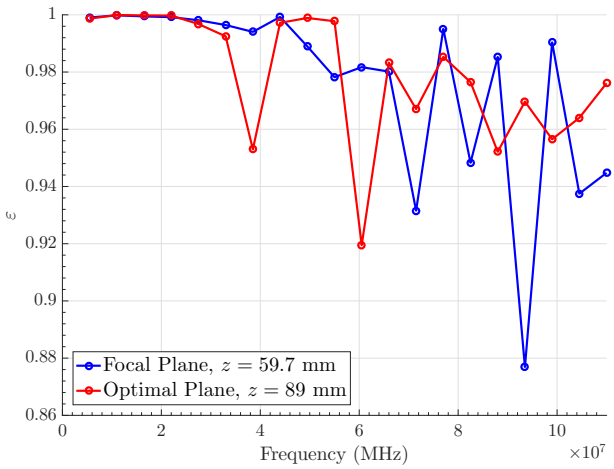

Fig. 5: Spatial-averaging errors at computed at focal plane, and post-focally at $z = 89$ mm.

IV. Discussion and Conclusion

The uncertainty associated with spatial-averaging for a nonlinear field is defined and calculated for each harmonic component. One may assume that for a focused field, high-harmonics components will be more localised, and thus will always have a greater spatial-averaging error and that this would lead to an underestimate of the field strength. However, both the measured and the simulated spatial-averaging errors show that the errors do not always decrease with frequency. The reason for this is that the analysis presented is predicated on the fact that the high frequency components are generated by nonlinear propagation. This is significant as the axial maxima of the higher harmonic components occur beyond the maximum of the peak positive pressure. Thus, for these high-frequency components, the acoustic field may not yet be fully convergent [10] and, as such, when averaged over the area of the measurement device, contain secondary maxima which result in a reduced spatial-averaging error.

The discretization error in the approximation of the area of the reference hydrophone with the test hydrophone was calculated to be 1%. The discretization error in the computation of the area of the reference hydrophone was less than 0.01%. Due to approximations in the operator splitting method, the largest error in the numerical simulation was $\mathcal{O}(\Delta z)$, but due to the small step sizes chosen, this was small.

Methods for correcting for spatial-averaging errors, such as those given in IEC 62127-1 [11], assume that the nominal and effective areas are equal. These may be different due to poling, irregular thickness or non-uniformity of the poled region of the piezoelectric element. To ascertain the effective area, first the directivity $D(f,\theta)$ is measured for a given frequency f and the angle of incident of a plane wave θ. Then, for a uniform circular element exposed to a coherent field in a uniform medium, the effective radius, a, can be computed via the relationship

$$D(f,\theta) = 2J_1(x)/x \tag{6}$$

where $J_1(\cdot)$ is the first order Bessel function, $x = ka\sin(\theta)$, $k = 2\pi f/c$ is the wavenumber and c is the speed of sound in the medium. However, at high frequencies the potential discrepancy between effective and nominal area is negligible – see [12, Fig. 5]. Thus, at the frequencies consider here, it is a justifiable to assume that the spatial-averaging error can be computed using the nominal area.

Acknowledgment

D.S. and S.R. gratefully acknowledge funding of the National Measurement System by the UK Department for Business, Energy & Industrial Strategy.

References

[1] N. C. Chaggares, O. Ivanytskyy, and G. Pang, "Design of a 30μm aperture membrane hydrophone for the measurement and characterization of high frequency ultrasound," in *Ultrasonics Symposium (IUS), 2016 IEEE International*. IEEE, 2016, pp. 1–6.

[2] R. A. Smith and D. R. Bacon, "A multiple-frequency hydrophone calibration technique," *J. Acoust. Soc. Am.*, vol. 87, no. 5, pp. 2231–2243, 1990.

[3] R. C. Preston, S. P. Robinson, B. Zeqiri, T. J. Esward, P. N. Gélat, and N. D. Lee, "Primary calibration of membrane hydrophones in the frequency range 0.5 MHz to 60 MHz," *Metrologia*, vol. 36, no. 4, pp. 331–343, 1999.

[4] P. N. Gélat, R. C. Preston, and A. Hurrell, "A theoretical model describing the transfer characteristics of a membrane hydrophone and validation," *Ultrasonics*, vol. 43, no. 5, pp. 331–341, 2005.

[5] K. A. Wear, P. M. Gammell, S. Maruvada, Y. Liu, and G. R. Harris, "Time-delay spectrometry measurement of magnitude and phase of hydrophone response," *IEEE Trans. Ultrason., Ferroelect., Freq. Contr.*, vol. 58, no. 11, pp. 2325–2333, 2011.

[6] A. Hurrell and S. Rajagopal, "The practicalities of obtaining and using hydrophone calibration data to derive pressure waveforms," *IEEE Trans. Ultrason., Ferroelect., Freq. Contr.*, vol. 64, no. 1, pp. 126–140, 2017.

[7] M. F. Hamilton and D. T. Blackstock, *Nonlinear Acoustics*. San Diego, CA: Academic Press, 1998.

[8] J. E. Soneson, "A User-Friendly Software Package for HIFU Simulation," in *8th Int. Symp. Therapeutic Ultrasound*, ser. ASME Conf. Proc., E. S. Ebbini, Ed., vol. 1113, 2009, pp. 165–169.

[9] W. Bich, M. Cox, R. Dybkaer, C. Elster, W. T. Estler, B. Hibbert, H. Imai, W. Kool, C. Michotte, and L. Nielsen, "Revision of the "Guide to the Expression of Uncertainty in Measurement"," *Metrologia*, vol. 49, no. 6, pp. 702–705, 2012.

[10] N. Jiménez, F. Camarena, J. Redondo, V. Sánchez-Morcillo, Y. Hou, and E. E. Konofagou, "Time-domain simulation of ultrasound propagation in a tissue-like medium based on the resolution of the nonlinear acoustic constitutive relations," *Acta Acustica united with Acustica*, vol. 102, no. 5, pp. 876–892, 2016.

[11] "Ultrasonics - Hydrophones - Part 1: Measurement and characterization of medical ultrasonic fields up to 40 MHz," International Electrotechnical Commission, Geneva, CH, Standard, Aug. 2007.

[12] R. A. Smith, "Are hydrophones of diameter 0.5 mm small enough to characterise diagnostic ultrasound equipment?" *Phys. Med. Biol.*, vol. 34, no. 11, pp. 1593–1607, 1989.